THE QUASI-BICIRCULAR PROBLEM FOR THE EARTH-MOON-SUN PARAMETERS

M.A. ANDREU and C. SIMÓ
Dept. Matemàtica Aplicada i Anàlisi, Univ. Barcelona,
Gran Via 585, 08007 Barcelona, Spain.
e-mails: mangel@maia.ub.es, carles@maia.ub.es

Abstract. The quasi-bicircular problem is a restricted four body problem where three masses are revolving in a quasi-bicircular motion (that is, a coherent motion close to circular), the fourth mass being small and not influencing the motion of the three primaries. A quasi-bicircular solution of the three body problem is computed for the Earth-Moon-Sun parameters. Then, the Hamiltonian governing the motion of the fourth particle under the gravitational influence of the first three masses is derived. Some resonant periodic orbits around L_1 and L_2 are shown. The system is reduced to an approximate center manifold and the periodic orbit found are used to check the range of validity of the approximation.

Keywords: Three body problem, four body problem, quasi-bicircular problem, Earth-Moon-Sun system.

1. Introduction

We are interested in the dynamics of the motion of a spacecraft in the Earth-Moon-Sun system and specially interested in the dynamics around the collinear points of the Earth-Moon system. The study of this dynamical system can be useful for future space missions. For instance, Halo orbits around the translunar libration point have been proposed as a mean to establish a continuous communications link between the Earth and the hidden side of the Moon (Farquhar, 1970).

To study the neighbourhood of the libration points of the Earth-Moon system, several models has been used in (Mohn et al., 1967), (Kolenkiewicz et al., 1968) and (Scheeres et al., 1992). One of the models that has been widely used is the Bicircular Problem ((Wiesel, 1984), (Gómez et al., 1987) and (Jorba, 1999)). This model is a restricted four body problem. It considers the Earth and the Moon moving in circular orbits around their barycenter which is also moving in circular orbit around the Sun. Nevertheless this model is not coherent because the motion of the three primaries is not a solution of the three body problem (3BP). The existence of the Sun modifies the Earth-Moon distance and therefore it can not be constant. This is specially important if we are interested in the motion near the collinear libration points.

In the next sections we are going to derive a coherent model close to the Bicircular Problem. This means that we will find a quasi-bicircular solution of the 3BP for Earth-Moon-Sun, and then we will be able to write the equations of the motion of a spacecraft subjected to the gravitational attraction of these bodies. The resulting system of equations has periodic dependence with respect to time, the period being equal to the synodic period of the Sun in the Earth-Moon system. Alternatively, the Hamiltonian with 3 DOF and time periodic dependence is given. The quasi-bicircular problem (QBCP) has been useful to start understanding the neighbourhood of the L_2 point of the real Earth-Moon system. For instance, in (Andreu et al., 1999a) and (Andreu, 1999) quasi-periodic Halo orbits of the QBCP were used as initial guess to compute Halo orbits of the JPL ephemeris model for long time span.

After deriving the model some periodic orbit whose frequency is resonant with the one of the system. In particular, we display some periodic orbits which, in the RTBP, correspond to planar Lyapunov, vertical Lyapunov and Halo periodic orbits. The results are presented in section 4.

The collinear points of the RTBP are known to be unstable. This instability is inherited by the QBCP around L_1 and L_2. To skip this instability from the equations of motion it is convenient to reduce the flow to the center manifold. On this manifold one has a Hamiltonian with 2 DOF keeping the time-periodic dependence. This is done in section 5. The reduction is formal and, in general (see (Jorba, in preparation)) it is not convergent, even if the frequencies satisfy suitable Diophantine conditions. To check the domain where the approximate center manifold provides a good approximation to the real one, periodic orbits corresponding to the ones obtained before are computed on the reduced manifold. Some conclusions are drawn in section 5. Some discussion followed by an outlook on future work is presented at the end of the paper.

2. Quasi-bicircular solution of the three body problem

Consider three particles E, M and S moving under their mutual gravity attraction. Let B the barycenter of the system and B_{em} the one of the particles E and M. We are interested in having a planar solution of the 3BP in such a way that E and M around B_{em}, and B_{em} and S around B, are moving close to circular orbits. This is called a quasi-bicircular solution of the 3BP.

In our case, the particles are Earth, Moon and Sun, with masses $1-\mu$, μ and m_s, respectively. The units of mass, time and length are

taken in such a way that the gravitational constant, the Earth-Moon distance and their mean motion are equal to 1. The mean distance from B_{em} to the Sun is a_s. The mean motion of B_{em} around the Sun is n_s, so the frequency of the Sun respect to the Earth-Moon system is $\omega_s = 1 - n_s$. In this work, the values used for these parameters are

$$\mu = 0.0121505816 \ , \qquad a_s = 388.81114 \ ,$$
$$\omega_s = 0.925195985520347 \ , \qquad m_s = n_s^2 \, a_s^3 - 1 \simeq 328900.54 \ .$$

The existence of quasi-bicircular solutions of the 3BP was proven in (Siegel et al., 1971) for any value of the mass parameters μ and m_s, at least for small values of the quotient $1/a_s$.

We consider the Jacobi formulation of the 3BP using the relative position vectors $\vec{r}$ and $\vec{R}$ (see figure 1). The equations of the motion can be written in complex notation, using z and Z instead of $\vec{r}$ and $\vec{R}$ (see (Marchal, 1990)). They are

$$\ddot{z} = -\frac{z}{r^3} + m_s \left(\frac{Z - \mu z}{r_{es}^3} - \frac{Z + (1-\mu) z}{r_{ms}^3} \right) \ , \tag{1}$$

$$\ddot{Z} = -(1 + m_s) \left(\mu \, \frac{Z + (1-\mu) z}{r_{ms}^3} + (1-\mu) \, \frac{Z - \mu z}{r_{es}^3} \right) \ , \tag{2}$$

where $r = |z|$, $r_{ms} = |Z + (1-\mu) z|$ and $r_{es} = |Z - \mu z|$. We want a solution of (1) and (2) with

$$z \simeq e^{it} \ , \qquad Z \simeq a_s e^{i n_s t} \ .$$

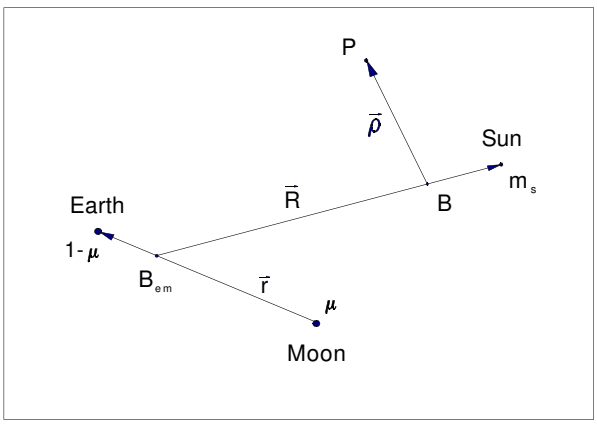

Figure 1. Quasi-bicircular problem in an inertial frame of reference.

Here, we are assuming that Moon, Earth and Sun are on the real axis at $t = 0$. It is possible to find such a solution as

$$z = e^{it} \sum_{j=-\infty}^{+\infty} b_j e^{ij\omega_s t} , \qquad Z = a_s e^{in_s t} \sum_{j=-\infty}^{+\infty} c_j e^{ij\omega_s t} , \qquad (3)$$

being $b_j, c_j \in I\!R$. For this purpose, let us first introduce the parameter $\epsilon_s = 1/a_s \simeq 1/388.8$. We note that $m_s \simeq 2.1756\epsilon_s^{-2}$. This suggests to rewrite (1) and (2) by replacing a_s by $1/\epsilon$ and m_s by $2.1756\epsilon^{-2}$, then to look for a solution of the form

$$z = e^{it} \left(1 + \sum_{k\geq 1} \epsilon^k u_k\right) , \qquad Z = a_s e^{in_s t} \left(1 + \sum_{k\geq 1} \epsilon^k v_k\right) ,$$

where u_k and v_k are trigonometric polynomials with basic frequency ω_s. After computing u_k and v_k, adding all the terms in powers of ϵ, we will get the coefficients b_j and c_j of the expressions (3). Substituting into the differential equations (1) and (2) and equating terms of the same order in ϵ, the polynomials u_k and v_k can be obtained recursively. Finally we will set $\epsilon = \epsilon_s$ to obtain the solution of the equation with the correct values of the parameters. Checks of the validity of the expansions up to $\epsilon = \epsilon_s$ are provided.

To obtain u_m and v_m, assume that $u_1, v_1, u_2, v_2, \ldots, u_{m-1}, v_{m-1}$ are known. The left hand side of (1) is

$$\ddot{z} = e^{it} \left(-1 + \sum_{k=1}^{m} \epsilon^k (\ddot{u}_k + 2i\dot{u}_k - u_k)\right) ,$$

and then

$$\ddot{z}|_m = e^{it}(\ddot{u}_m + 2i\dot{u}_m - u_m) ,$$

where $|_m$ means terms of order ϵ^m. In a similar way, from the left hand side of (2) we get

$$\ddot{Z}\Big|_m = a_s e^{in_s t}(\ddot{v}_m + 2in_s\dot{v}_m - n_s^2 v_m) .$$

On the right part of (1) and (2), there are several terms:

$$\frac{z}{r^3} = e^{it} \left(1 + \sum_{k=1}^{m} \epsilon^k u_k\right)^{-1/2} \left(1 + \sum_{k=1}^{m} \epsilon^k \overline{u}_k\right)^{-3/2} , \qquad (4)$$

and so

$$\frac{z}{r^3}\Big|_m = e^{it} \left(-\frac{1}{2}u_m - \frac{3}{2}\overline{u}_m + \text{ k. t.}\right) ,$$

where k.t. means "known terms" which can be computed from the previous u_k's and $\overline{x}$ denotes the complex conjugate of x. On the right hand side of the equality we also have

$$\frac{Z-\mu z}{r_{es}^3} = \frac{e^{in_s t}}{a_s^2}\left(1+\sum_{k=1}^{m}\epsilon^k(v_k-\mu e^{int}u_{k-1})+O(\epsilon^{m+1})\right)^{-1/2} \left(1+\sum_{k=1}^{m}\epsilon^k(\overline{v}_k-\mu e^{int}\overline{u}_{k-1})+O(\epsilon^{m+1})\right)^{-3/2} , \quad (5)$$

and then, the terms of order ϵ^m are

$$\left.\frac{Z-\mu z}{r_{es}^3}\right|_m = \frac{e^{it}}{a_s^2}e^{-i\omega_s t}(-\frac{1}{2}v_m-\frac{3}{2}\overline{v}_m+\text{ k. t.}) .$$

Following a similar procedure, we also arrive at

$$\left.\frac{Z-(1-\mu)z}{r_{ms}^3}\right|_m = \frac{e^{it}}{a_s^2}e^{-i\omega_s t}(-\frac{1}{2}v_m-\frac{3}{2}\overline{v}_m+\text{ k. t.}) .$$

Note that in (1) the terms containing Z have a factor m_s in front of them, but as they also have the factor $1/a_s^2$, the total contribution, m_s/a_s^2, is $O(1)$. Consequently, we only should solve the linear differential system:

$$\ddot{u}_m+2i\dot{u}_m-\frac{3}{2}u_m-\frac{3}{2}\overline{u}_m = P_m(e^{i\omega_s t}) , \quad (6)$$

$$\ddot{v}_m+2in_s\dot{v}_m-\frac{3}{2}n_s^2v_m-\frac{3}{2}n_s^2\overline{v}_m = Q_m(e^{i\omega_s t}) , \quad (7)$$

where P_m and Q_m are polynomials depending on the precedent u_k and v_k for $k=1,\ldots,m-1$. These polynomials have real coefficients and integer exponents as will be proved later on.

If P_m is known and

$$P_m(e^{i\omega_s t}) = \sum_{|j|\le J} p_{mj}e^{ij\omega_s t} ,$$

where J is finite and depends on m (see prop. 1), a particular solution of (6) is of the form:

$$u_m = \sum_{|j|\le J} u_{mj}e^{ij\omega_s t} .$$

Inserting u_m in (6) we proceed to determine the u_{mj} coefficients. The independent term $u_{m0}=-p_{m0}/3$ is readily found. If $|j|\neq 0$ we have

$$(\gamma_j+\delta_j)u_{m,-j}-\frac{3}{2}u_{mj}=p_{m,-j} , \qquad -\frac{3}{2}u_{m,-j}+(\gamma_j-\delta_j)u_{mj}=p_{mj} , \quad (8)$$

where $\gamma_j = -(j\omega_s)^2 - 3/2$ and $\delta_j = 2j\omega_s$.

For (7) we proceed in the same way and obtain $v_{m0} = -q_{m0}/(3n_s^2)$ and, for $|j| \neq 0$,

$$(\hat{\gamma}_j + \hat{\delta}_j)v_{m,-j} - \frac{3}{2}n_s^2 v_{mj} = q_{m,-j} \ , \qquad -\frac{3}{2}n_s^2 v_{m,-j} + (\hat{\gamma}_j - \hat{\delta}_j)v_{mj} = q_{mj} \ , \tag{9}$$

where $\hat{\gamma}_j = -(j\omega_s)^2 - 3n_s^2/2$ and $\hat{\delta}_j = 2j\omega_s n_s$.

The determinants of systems (8) and (9) ($(j\omega_s)^2((j\omega_s)^2 - 1)$ and $(j\omega_s)^2((j\omega_s)^2 - n_s^2)$) are always different from zero. The smallest values are reached for $j = 1$.

PROPOSITION 1. *The polynomials P_m and Q_m of the equations (6) and (7) have real coefficients, integer exponents and their degrees satisfy*

$$deg(P_m) \leq 2\,m \ , \qquad deg(Q_m) \leq 2\,m - 2 \ , \qquad \forall m \geq 1 \ .$$

Proof. First of all we compute u_1 and v_1. From

$$P_1 = \left(\frac{1}{2} + \frac{3}{2}\,e^{-2i\omega_s t}\right)\frac{m_s}{a_s^2} \ , \qquad Q_1 = 0 \ ,$$

we get $v_1 = 0$ and

$$u_1 = \left(-\frac{1}{6} - \frac{24\omega_s^2 + 24\omega_s + 9}{64\omega_s^4 - 16\omega_s^2}\,e^{-2i\omega_s t} + \frac{9}{64\omega_s^4 - 16\omega_s^2}\,e^{2i\omega_s t}\right)\frac{m_s}{a_s^2} \ .$$

Hence we have $deg(P_1) = 2$ and $deg(Q_1) = 0$. Now, we proceed by induction. Assume that $deg(P_k) \leq 2\,k$ and $deg(Q_k) \leq 2\,k - 2$ for all $k = 1, \ldots, m-1$. We want to see that this is also true for $k = m$. It is clear that u_k and v_k are trigonometric polynomials of the same degree than P_k and Q_k. Looking at (1) and (2) and formulas (4) and (5), it is easy to see that $deg(P_m) \leq 2\,m$ and $deg(Q_m) \leq 2\,m - 2$. We only want to remark that in (5) some terms of degree $2m - 1$ are involved. When computing $\dfrac{Z - (1-\mu)z}{r_{ms}^3}$ and $\dfrac{Z - \mu z}{r_{es}^3}$ some terms of that degree appear, but when adding both in (2), those terms cancel, and so $deg(Q_m) \leq 2\,m - 2$.

In order to study the convergence of the solution, the maximum coefficient of each term $\epsilon^k u_k$ and $\epsilon^k v_k$ is given. This maximum is denoted by $\|\cdot\|_m$ and table I shows it for some degrees. We see that $\|\epsilon^k u_k\|_m$ and $\|\epsilon^k v_k\|_m$ show a very regular behaviour. The quotient between each term and the next one is approximately 2.6. We decided to compute the solution up to order 30. At this point the round-off errors are certainly

Table I. Maximum coefficient of $\epsilon^k u_k$ and $\epsilon^k v_k$ for some values of k.

k	$\|\epsilon^k u_k\|_m$	$\|\epsilon^k v_k\|_m$
5	1.39189e–05	2.43716e–13
10	1.15466e–07	2.02341e–15
15	9.58163e–10	1.67902e–17
20	7.95281e–12	1.39358e–19
25	6.60176e–14	1.37143e–21
30	5.48047e–16	1.38933e–23

Table II. Coefficients of the quasi-bicircular motion of the Earth-Moon-Sun system. All the not printed coefficients are less than 10^{-10}.

j	b_j	c_j
–6	2.444541403181094e−09	
–5	4.604798391613412e−09	
–4	1.545864413695503e−07	
–3	7.360514539804505e−06	
–2	−8.688592707298765e−03	2.626400997925652e−10
–1	−4.483846462932090e−04	−2.481941620308044e−12
0	9.990930211448791e−01	1.000000018781437e+00
1	1.607506070429252e−04	
2	1.514503555873263e−03	
3	1.474833975440193e−07	
4	5.874877029010216e−06	
5	−1.212071450975000e−09	
6	3.001784387420479e−08	
7	−1.788769852254027e−11	
8	1.752254234365158e−10	

bigger than the truncation errors. Table II shows the coefficients b_j and c_j of the solution.

3. Quasi-bicircular problem

The QBCP is a restricted four body problem, where the first three masses are moving in a quasi-bicircular movement and the fourth is an

infinitesimal mass. In this section we are going to derive the Hamiltonian and the equations of the motion of the fourth particle under the gravitational influence of the other three masses.

Consider an inertial reference frame centered at the center of masses B. Let $\vec{r}$ and $\vec{R}$ be the vectors introduced in section 2 in the Jacobi decomposition (see again figure 1). We suppose that the motion of the three primaries stands on a plane. This plane can be considered the xy plane, without loss of generality. In this reference frame, the position vectors of the Earth, Moon and Sun are the following:

$$\begin{aligned}
\vec{\rho}_e &= -\frac{m_s}{1+m_s}\,\vec{R} + \mu\,\vec{r}\,, \\
\vec{\rho}_m &= -\frac{m_s}{1+m_s}\,\vec{R} - (1-\mu)\,\vec{r}\,, \\
\vec{\rho}_s &= \frac{1}{1+m_s}\,\vec{R}\,,
\end{aligned}$$

where $\vec{r}(t) = (\mathrm{Re}\, z, \mathrm{Im}\, z, 0)$, $\vec{R}\,(t) = (\mathrm{Re}\, Z, \mathrm{Im}\, Z, 0)$, $r = |\vec{r}|$ and $R = |\vec{R}\,|$.

Now, we are going to perform a change of coordinates. The change consists in a translation, a rotation and an homothetic transformation. The translation sends the origin of coordinates to the Earth-Moon barycenter. The rotation puts the Earth and the Moon on the x axis. Finally, the homothetic transformation makes the Earth-Moon distance constant. This is a rotating pulsating reference frame. The new coordinates are related to the old ones by the formula

$$\vec{q} = \frac{1}{r^2}\, C^T \left(\vec{\rho} + \frac{m_s}{1+m_s}\,\vec{R} \right)\,,$$

where

$$C = \begin{pmatrix} r_1 & -r_2 & 0 \\ r_2 & r_1 & 0 \\ 0 & 0 & r \end{pmatrix}\,.$$

In this reference frame, the coordinates of the Earth, Moon and Sun become

$$\vec{q}_{\,e} = (\mu, 0, 0)^T\,, \qquad \vec{q}_{\,m} = (\mu - 1, 0, 0)^T\,, \qquad \vec{q}_{\,s} = \frac{1}{r^2}\, C^T\, \vec{R}\,.$$

In this way, the Earth and the Moon are located at the same place as in the RTBP. This is useful to make comparisons and we can also think about the QBCP as a perturbation of the RTBP.

Using the new coordinates, the potential energy is

$$U = -\frac{1-\mu}{r\,\|\vec{q}_{\,e} - \vec{q}\,\|} - \frac{\mu}{r\,\|\vec{q}_{\,m} - \vec{q}\,\|} - \frac{m_s}{r\,\|\vec{q}_{\,s} - \vec{q}\,\|}\,.$$

The kinetic energy

$$T = \frac{1}{2} < \dot{\vec{\rho}}, \dot{\vec{\rho}} > \ .$$

can be transformed taking into account that

$$\dot{\vec{\rho}} = -\frac{m_s}{1+m_s}\,\dot{\vec{R}} + \dot{C}\vec{q} + C\dot{\vec{q}}\ ,$$

and we get

$$T = \frac{1}{2}r^2\dot{\vec{q}}^2 + \vec{q}^T\dot{C}^T C\dot{\vec{q}} + \frac{1}{2}\vec{q}^T\dot{C}^T\dot{C}\vec{q} - \frac{m_s}{1+m_s}\dot{\vec{R}}^T\dot{C}\vec{q} - \\ -\frac{m_s}{1+m_s}\dot{\vec{R}}^T C\dot{\vec{q}} + \frac{m_s^2}{2(1+m_s)^2}\dot{\vec{R}}^2\ .$$

The momentum is defined as

$$\vec{p} = \frac{\partial T}{\partial \dot{\vec{q}}} = r^2\dot{\vec{q}} + C^T\dot{C}\vec{q} - \frac{m_s}{1+m_s}C^T\dot{\vec{R}}\ ,$$

and so

$$\dot{\vec{q}} = \frac{1}{r^2}\left(\vec{p} - C^T\dot{C}\vec{q} + \frac{m_s}{1+m_s}C^T\dot{\vec{R}}\right)\ .$$

Substituting this expression in the kinetic energy, by a straightforward calculation, we arrive at

$$T = \frac{1}{2r^2}\,\vec{p}^{\,2}\ .$$

Then, the Hamiltonian is

$$H = \vec{p}\,\dot{\vec{q}} - T + U = \\ = \frac{1}{2r^2}\vec{p}^{\,2} - \frac{1}{r^2}\vec{p}\,C^T\dot{C}\vec{q} + \frac{m_s}{1+m_s}\,\frac{1}{r^2}\dot{\vec{R}}^T C\vec{p} + U\ ,$$

and the Hamiltonian equations are

$$\dot{\vec{q}} = \frac{\partial H}{\partial \vec{p}} = \frac{1}{r^2}\vec{p} - \frac{1}{r^2}C^T\dot{C}\vec{q} + \frac{m_s}{1+m_s}\,\frac{1}{r^2}C^T\dot{\vec{R}}\ , \tag{10}$$

$$\dot{\vec{p}} = -\frac{\partial H}{\partial \vec{q}} = \frac{1}{r^2}\dot{C}^T C\vec{p} - \frac{\partial U}{\partial \vec{q}}\ . \tag{11}$$

However, we are going to modify the Hamiltonian slightly. The system of first order differential equations (10) and (11) is equivalent to the second order equation

$$\frac{d}{dt}(r^2\dot{\vec{q}} + C^T\dot{C}\vec{q}) = \frac{1}{r^2}\dot{C}^T C(r^2\dot{\vec{q}} + C^T\dot{C}\vec{q}) + \frac{m_s}{1+m_s}C^T\ddot{\vec{R}} - \frac{\partial U}{\partial \vec{q}}\ .$$

Therefore, we can redefine the momentum as

$$\vec{p} = r^2 \dot{\vec{q}} + C^T \dot{C} \vec{q} \ ,$$

and then the first order differential equations are

$$\begin{aligned} \dot{\vec{q}} &= \frac{1}{r^2} \left(\vec{p} - C^T \dot{C} \vec{q} \right) , \\ \dot{\vec{p}} &= \frac{1}{r^2} \dot{C}^T C \vec{p} + \frac{m_s}{1+m_s} C^T \ddot{\vec{R}} - \frac{\partial U}{\partial \vec{q}} \ . \end{aligned}$$

Finally, the Hamiltonian corresponding to these equations is

$$H = \frac{1}{2r^2} \vec{p}^{\,2} - \frac{1}{r^2} \vec{p} C^T \dot{C} \vec{q} - \frac{m_s}{1+m_s} \ddot{\vec{R}}^{\,T} C \vec{q} + U \ . \tag{12}$$

To write the above Hamiltonian in a more suitable way, the expressions of z and Z of the previous section are used to define the periodic functions $\alpha_k(t)$:

$$\alpha_1 = \frac{1}{r^2} \ , \qquad \alpha_2 = -\frac{Re(\dot{z}\overline{z})}{r^2} \ , \qquad \alpha_3 = \frac{Im(\dot{z}\overline{z})}{r^2} \ ,$$

$$\alpha_4 = -\frac{m_s}{1+m_s} Re(\ddot{Z}\overline{z}) \ , \quad \alpha_5 = -\frac{m_s}{1+m_s} Im(\ddot{Z}\overline{z}) \ , \quad \alpha_6 = \frac{1}{r} \ ,$$

$$\alpha_7 = \frac{1}{r^2} Re(Z\overline{z}) \ , \qquad \alpha_8 = \frac{1}{r^2} Im(Z\overline{z}) \ .$$

We realize that all the α_k functions are either even (α_1, α_3, α_4, α_6, α_7) or odd (α_2, α_5, α_8). More concretely

$$\alpha_k(t) = \alpha_{k0} + \sum_{j \geq 1} \alpha_{kj} \cos(j\theta) \ , \qquad \text{for } k = 1, 3, 4, 6, 7, \tag{13}$$

$$\alpha_k(t) = \sum_{j \geq 1} \alpha_{kj} \sin(j\theta) \ , \qquad \text{for } k = 2, 5, 8, \tag{14}$$

with $\alpha_{kj} \in \mathbb{R}$, which are shown in table III and $\theta = \omega_s t$.

Let $\vec{q} = (x, y, z)^T$ be the position vector and $\vec{p} = (p_x, p_y, p_z)^T$ the momentum. We hope that there is no confusion between the coordinate z and the previous use of z. The Hamiltonian (12) can be written as

$$\begin{aligned} H = \ & \frac{1}{2} \alpha_1 (p_x^2 + p_y^2 + p_z^2) + \alpha_2 (p_x x + p_y y + p_z z) + \alpha_3 (p_x y - p_y x) + \\ & + \alpha_4 x + \alpha_5 y - \alpha_6 \left(\frac{1-\mu}{q_{pe}} + \frac{\mu}{q_{pm}} + \frac{m_s}{q_{ps}} \right) \ , \end{aligned} \tag{15}$$

Table III. A sample of Fourier coefficients of α_k functions. All the coefficients not printed here are less than 10^{-6}.

j	α_1	c	α_2	s	α_3	c
0	1.001841608925e+00				1.000000000000e+00	
1	5.767517726198e−04		−2.644376028500e−04		5.634125997554e−04	
2	1.438777025508e−02		−1.328686903400e−02		1.889687440173e−02	
3	−2.630362974972e−06		9.386093208090e−06		−9.911758802567e−06	
4	1.176278356119e−04		−1.218509057517e−04		1.568708136031e−04	
5	−8.068581391006e−08		1.522127598557e−07		−1.707762576173e−07	
6	9.843249766501e−07		−1.072102664278e−06		1.319613679707e−06	
j	α_4	c	α_5	s	α_6	c
0	−9.755242327485e−04				1.000907457708e+00	
1	2.154764362707e+00		−2.192570751040e+00		2.870921750053e−04	
2	3.657484468969e−04		−3.337210485473e−04		7.187177998613e−03	
3	3.295673376167e−03		−3.295001430201e−03		−2.351183147213e−06	
4	3.301031400812e−07		−3.100635053053e−07		4.585758971122e−05	
5	1.278840687376e−05		−1.277777336854e−05		−3.848683620107e−08	
j	α_7/a_s	c	α_8/a_s	s		
0	−1.623942556792e−04					
1	9.993640159328e−01		−1.002398556851e+00			
2	4.467233637764e−04		−4.460466761118e−04			
3	8.700645952865e−03		−8.707817596590e−03			
4	4.050392088510e−07		−4.001651373501e−07			
5	7.552151126648e−05		−7.555294511283e−05			

where

$$\begin{aligned} q_{pe}^2 &= (x-\mu)^2 + y^2 + z^2 \ , \\ q_{pm}^2 &= (x-\mu+1)^2 + y^2 + z^2 \ , \\ q_{ps}^2 &= (x-\alpha_7)^2 + (y-\alpha_8)^2 + z^2 \ . \end{aligned}$$

The Hamiltonian equations present two trivial symmetries:

$$\begin{aligned} S_1 &: (x, y, z, \dot{x}, \dot{y}, \dot{z}, t) \longleftrightarrow (x, y, -z, \dot{x}, \dot{y}, -\dot{z}, t) \ , \\ S_2 &: (x, y, z, \dot{x}, \dot{y}, \dot{z}, t) \longleftrightarrow (x, -y, z, -\dot{x}, \dot{y}, -\dot{z}, -t) \ . \end{aligned}$$

To check the second one it is necessary to take into account the parity properties of the α_k functions. The equations of the RTBP present also the same symmetries S_1 and S_2.

Comparing (15) with the Hamiltonian of the RTBP, we see that in that case the corresponding α coefficients are $\alpha_1 = \alpha_3 = \alpha_6 = 1$, $\alpha_2 = \alpha_4 = \alpha_5 = 0$ and the terms of the potential of the Sun do not appear. In the case of the Bicircular Problem, we also have $\alpha_1 = \alpha_3 = \alpha_6 = 1$, $\alpha_2 = 0$, but

$$\alpha_4 = \frac{m_s}{a_s^2}\cos\theta\ ,\quad \alpha_5 = -\frac{m_s}{a_s^2}\sin\theta\ ,\quad \alpha_7 = a_s\cos\theta\ ,\quad \alpha_8 = -a_s\sin\theta\ .$$

4. Periodic orbits around the L_1, L_2 collinear points

Periodic orbits of the QBCP have period equal to T or multiples of T. To look for periodic orbits of the QBCP, we start looking for periodic orbits of the RTBP with period pT/q, $p, q \in I\!N$. If an orbit has period pT/q, it can be considered as pT-periodic orbit travelled q times. We say that such orbit is in a p:q resonance. Later on, we will show that periodic orbits can be used to check the accuracy of the center manifold.

We are interested in periodic orbits around the collinear equilibrium points L_i, $i = 1, 2$. We have computed the two Lyapunov families of periodic orbits of the RTBP (the planar and the vertical one) emanating from the L_i points. We also have computed the Halo families bifurcating from the planar Lyapunov families. The planar families have been followed moving the initial condition from L_i up to the middle point of the L_i-Moon line. The families of vertical Lyapunov and Halo orbits have been followed up to the maximum z coordinate of them has reached the value of 0.5 units the L_i-Moon distance. In each family the p:q resonant orbits have been computed for $q \leq 8$. Table IV shows which resonances appear in each case.

Then, we consider the family of Hamiltonians

$$H = H_{RTBP} + \delta\,(H_{QBCP} - H_{RTBP})\ , \tag{16}$$

depending on the parameter δ and we compute families of periodic orbits of this Hamiltonian when varying δ. For $\delta = 0$ we have the Hamiltonian of the RTBP and for $\delta = 1$ the Hamiltonian of the QBCP. The main difference between RTBP and QBCP is that the first one is autonomous and the second one is non-autonomous. In the autonomous case, any point of a periodic orbit can be taken as initial point for any initial epoch. We study which points of the resonant periodic orbits can be continued leading to periodic orbits for small values of the parameter δ (see (Simó, 1990) and (Andreu, 1999)). Table IV also shows how many orbits bifurcate from each resonant orbit of the RTBP.

Table IV. Main resonances around L_1 and L_2. N=Number of orbits bifurcating from the orbits of the RTBP.

		Resonance	N	Label
L_1	Planar Lyapunov	2:5	4	2
		3:7	6	3
		1:2	2	4
	Vertical Lyapunov	none		
	Halo	none		
L_2	Planar Lyapunov	1:2	4	6
	Vertical Lyapunov	none		
	Halo	1:2	4	7

To follow the families of periodic orbits when varying δ, a continuation method has been used. For orbits with period longer than T, it is also necessary to use a multiple shooting method (Stoer et al., 1980). We want to remark that the orbits around L_1 and L_2 are very unstable. A particle nearby a periodic orbit around L_i (i=1,2), each revolution around this point, the distance from the particle to the periodic orbit is roughly multiplied by 1000.

Periodic orbits bifurcating from the orbits of the RTBP have been continued up to the QBCP. The T-periodic orbits coming from the fixed points of the RTBP also have been computed. All these orbits are shown in figures 2 and 3. In these figures, the orbits of the RTBP are displayed with dotted lines, while the continuous lines correpond to the orbits of the QBCP. Bifurcating points from the autonomous orbit for $t = 0$ are marked with $\square$. Initial points of the orbits of the QBCP are marked with $\circ$ or $\times$ depending on their stability character inside the center manifold.

Most of the figures of periodic orbits show that the initial point of each orbit is close to the bifurcating point in the RTBP which generates it. But, this does not happen for the orbits labelled as (6) and (7). For example, in case of the orbit (6d), when the continuation parameter is increased, the initial point follows a long path starting at the point marked as D at ending at the point with label d. In the case of orbits labelled as (7), we notice that the orbit of the RTBP has four points of bifurcation. Increasing the continuation parameter, the points B and D go towards the point C, following a similar path to the plotted orbits. For the value $\epsilon \simeq 0.99833$ the branches from B and D disappear in a pitchfork bifurcation joining with the branch of C. For this reason,

only two orbits remain in the QBCP. For more periodic orbits, including periodic orbits around the other libration points, see (Andreu, 1999).

To study the stability of the periodic orbits, we use the stability parameters defined as

$$s_k = \lambda_k + 1/\lambda_k \ , \qquad k = 1, 2, 3 \ ,$$

where λ_k are the eigenvalues of the monodromy matrix of the periodic orbit, M. We recall that M is a 6×6 symplectic matrix and, consequently, if λ is an eigenvalue of M then $1/\lambda$ also does. The stability parameters of the computed periodic orbits are shown in table V. We notice that all the orbits have a very strong hyperbolic part. We also want to comment that to compute the parameter close to 2 of the orbits with period longer than T, it has been necessary to use quadruple precision.

Table V. Stability parameters of periodic orbits of the QBCP.

Label	s_1	s_2	s_3
1	4.6018213e+08	−1.9272794e+00	−1.9743038e+00
2a	1.0093836e+17	2.0000028e+00	1.6866650e+00
2b,d	1.0093737e+17	1.9999972e+00	1.6866649e+00
2c	1.0093836e+17	2.0000028e+00	1.6866650e+00
3a	3.2185380e+22	8.2984016e+00	2.0000002e+00
3b,f	3.2185378e+22	8.2984017e+00	1.9999998e+00
3c,e	3.2185380e+22	8.2984016e+00	2.0000002e+00
3d	3.2185378e+22	8.2984017e+00	1.9999998e+00
4a	5.6020544e+05	2.8751711e+00	2.0119296e+00
4b	5.5630422e+05	2.8781160e+00	1.9829068e+00
5	2.3971968e+06	1.9916366e+00	1.8350556e+00
6a	1.7294557e+06	1.9998183e+00	1.9089728e+00
6b,d	1.7347639e+06	2.0000025e+00	1.9068636e+00
6c	1.7347233e+06	1.9999987e+00	1.9068600e+00
7a	1.1381097e+06	2.0002929e+00	1.7358171e+00
7c	1.1308529e+06	1.9999994e+00	1.7292282e+00

5. Reduction to the center manifold

To have a full description of the dynamics of the QBCP in a big neighborhood around L_1 and L_2, we have computed the reduction of the

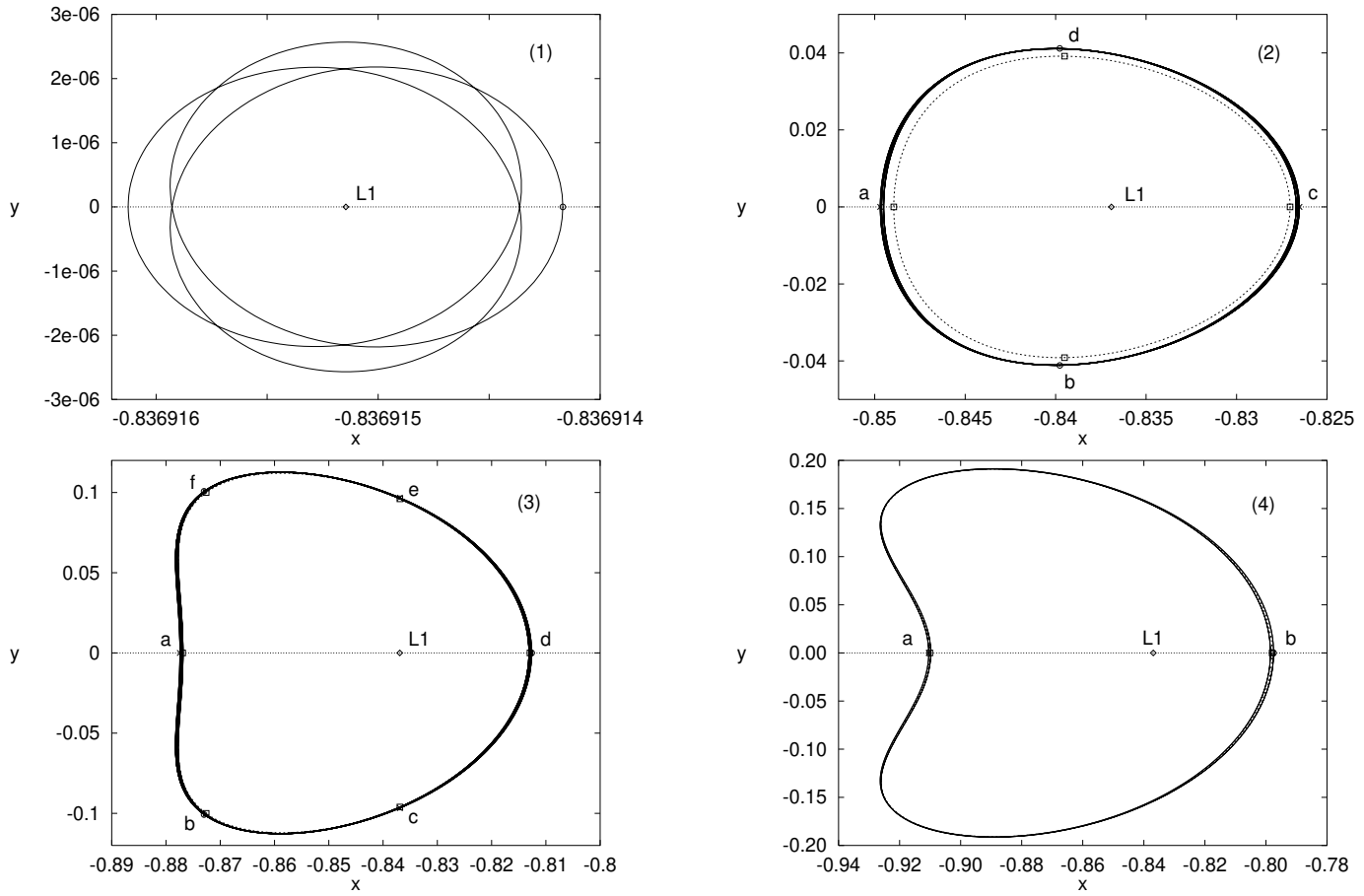

Figure 2. Periodic orbits around L_1. (1) Orbit substituting the equilibrium point. (2), (3) and (4) planar periodic orbits in resonances 2:5, 3:7 and 1:2, respectively.

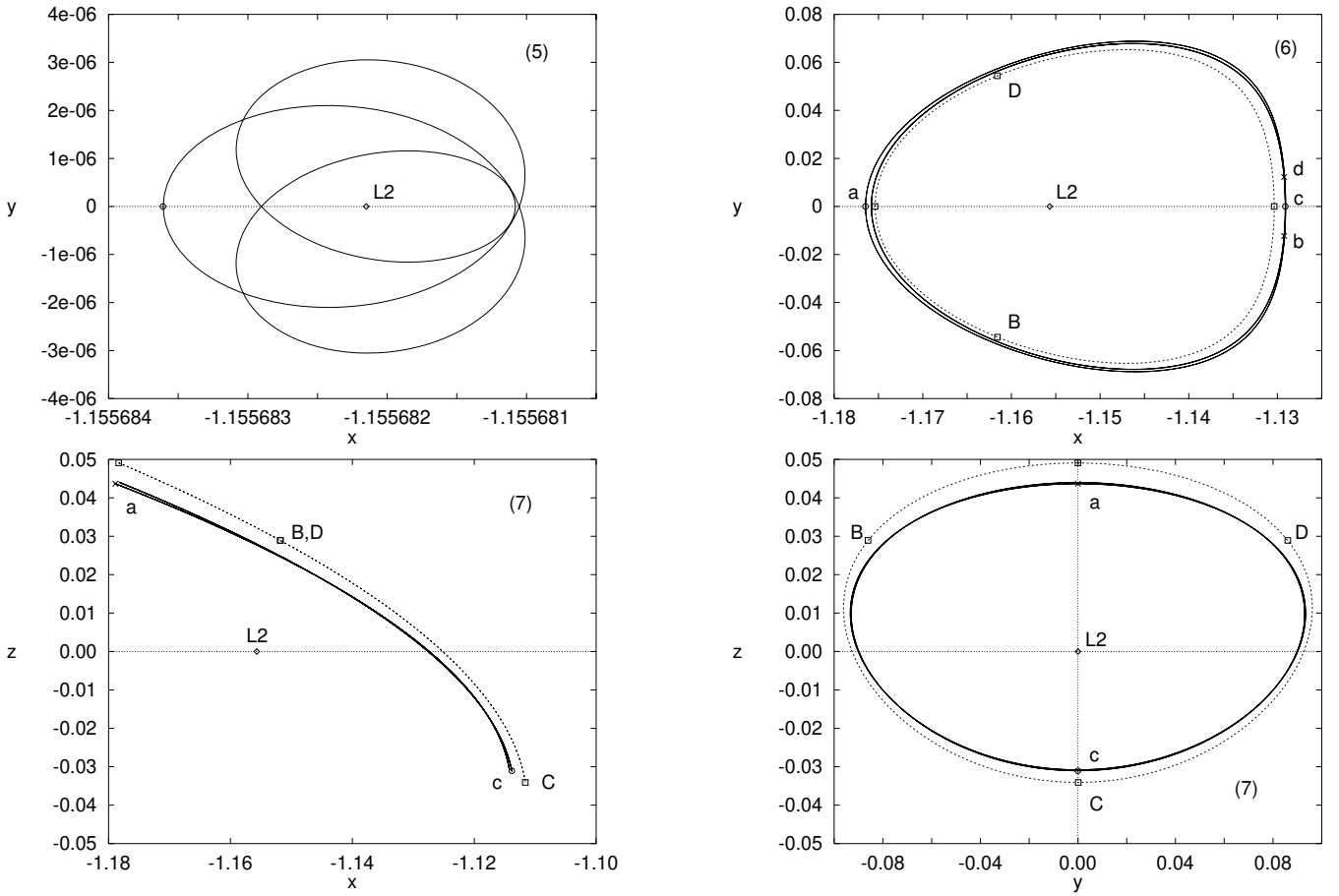

Figure 3. Periodic orbits around L_2. (5) Orbit substituting the equilibrium point. (6) planar periodic orbits in resonance 1:2. (7.1) and (7.2) are (x, z) and (y, z) projections of the 1:2 resonant Halo orbit.

Hamiltonian to the center manifold. In fact, we have only computed a polynomial approximation up to order 16, but it is suficient for our purpose. On the other hand, we recall that this reduction is not convergent in any open set. In next section we show two different ways to check the goodness of the approximation computed.

We want to summarize the process of reduction to the center manifold. For more details we refer to (Andreu, 1999). The Hamiltonian of the QBCP (15) can be expanded using Legendre polynomials as

$$H = \sum_{|k|\geq 1} (\sum_{j} h_{kj} e^{\sqrt{-1}\, j\theta}) x^{k_1} y^{k_2} z^{k_3} p_x^{k_4} p_y^{k_5} p_z^{k_6} \ , \tag{17}$$

where $h_{kj} \in \mathbb{C}$, k is the multiindex $(k_1, k_2, k_3, k_4, k_5, k_6)$, $|k| = \sum_i k_i$ and $\theta = \omega_s t$. In fact, for practical reasons, the expansion of the Hamiltonian is not computed now. It will be expanded after the computation of the Floquet change of variables. From now on, we rename the position as $x = (x_1, x_2, x_3)$ and the momentum $y = (y_1, y_2, y_3)$.

To perform canonical changes of variables, we use Lie's method. Given a generating function G, the new Hamiltonian is obtained by means of

$$\tilde{H} = H + \{H, G\} + \frac{1}{2!}\{\{H, G\}, G\} + \frac{1}{3!}\{\{\{H, G\}, G\}, G\} + \dots \ ,$$

where $\{\cdot, \cdot\}$ is the Poisson bracket.

To compute the reduction to the center manifold, we have done the following steps:

1. To cancel the terms of degree one of the Hamiltonian, we perform a translation to the periodic orbit which substitutes the equilibrium point $\mathrm{L_i}$, $i = 1, 2$ (orbits labelled in section 4 as (1) and (5), respectively). We notice that the translation depends on time. In this way, the origin of coordinates becomes a fixed point.

2. A symplectic Floquet change of variables is used to cancel the dependence on time of the second degree terms of the Hamiltonian and simultaneously, we get the matrix of the linear part of the Hamiltonian equations of the QBCP in Jordan form. It is

$$J_B = \left(\begin{array}{ccc|ccc} 0 & 0 & 0 & \omega_1 & 0 & 0 \\ 0 & \omega_2 & 0 & 0 & 0 & 0 \\ 0 & 0 & 0 & 0 & 0 & \omega_3 \\ \hline -\omega_1 & 0 & 0 & 0 & 0 & 0 \\ 0 & 0 & 0 & 0 & -\omega_2 & 0 \\ 0 & 0 & -\omega_3 & 0 & 0 & 0 \end{array}\right) \ ,$$

where we have used the values

	L_1	L_2
ω_1	$-4.38968497e{-}01$	$1.34709425e{-}02$
ω_2	$2.93720565e{+}00$	$2.16306748e{+}00$
ω_3	$4.22768254e{-}01$	$-6.02217885e{-}02$

We notice that the normal frequencies associated to the small periodic orbit around L_1 are $\omega_1 + 3\omega_s$ and $\omega_3 + 2\omega_s$. Moreover, they are very similar to the frequencies of the equilibrium point L_1 of the RTBP. In the case of L_2, the frequencies are $\omega_1 + 2\omega_s$ and $\omega_3 + 2\omega_s$.

3. We use the complexification change of variables given by

$$x_j = \frac{\tilde{x}_j + \sqrt{-1}\,\tilde{y}_j}{\sqrt{2}}\,, \qquad y_j = \frac{\sqrt{-1}\,\tilde{x}_j + \tilde{y}_j}{\sqrt{2}}\,,$$

for $j = 1, 3$, the non hyperbolic part of the Hamiltonian. The variables with tilde are the new ones, but, after the change, we rename the new variables with the same name that the old ones. The complexification is necessary to apply an efficient algorithm to put in partial normal form terms of the Hamiltonian of order greater than two. This partial normal form allows to reduce the Hamiltonian to the center manifold and to obtain a "simplified" expression for the reduced Hamiltonian.

4. Till now, it was not necessary to expand the Hamiltonian. The translation to the periodic orbit and the Floquet's change of variables are computed using the initial Hamiltonian. Then, we compose the three previous change of variables and the Hamiltonian (15) is expanded using the recurrences involving the Legendre polynomials.

5. To obtain the Hamiltonian reduced to the center manifold it is only necessary to cancel all the terms of degree 1 in the hyperbolic pair of varibles (x_2, y_2). Moreover, in order to get a final Hamiltonian as simple as possible, we cancel all the terms not depending on time, x_2 and y_2, as long as the divisor involved in the generating function is larger than 0.05. It is also possible to cancel all those terms which depend on time. Then, the generating functions G_3, G_4, ..., G_n to put the Hamiltonian in partial normal form up to order n can be computed explicitly (see (Andreu, 1999)). Once we have the Hamiltonian in partial normal form, the center manifold is simply $x_2 = y_2 = 0$.

6. In order to get the Hamiltonian in real coordinates, another change of variables must be applied. We call it *realification* and it is the inverse of the complexification done before. It is, for $j = 1, 3$,

$$x_j = \frac{\tilde{x}_j - \sqrt{-1}\,\tilde{y}_j}{\sqrt{2}}\,,$$
$$y_j = \frac{-\sqrt{-1}\,\tilde{x}_j + \tilde{y}_j}{\sqrt{2}}\,.$$

Using all these changes of variables, the Hamiltonian restricted to the center manifold around L_i (i=1,2) up to order 16 has been computed. It is of the form

$$H_{CM}^{(i)} = \frac{1}{2}\omega_1(x_1^2 + y_1^2) + \frac{1}{2}\omega_3(x_3^2 + y_3^2) + \sum_k h_k\, x_1^{k_1} y_1^{k_2} x_3^{k_5} y_3^{k_6}\,, \quad (18)$$

with $h_k \in \mathbb{R}$. Although there were some few terms leading to small divisors, they were also cancelled because they were not important (that is, their coefficients were small enough). So, with the reduction to the center manifold, we obtain an autonomous Hamiltonian. Let ψ_i, $i = 1, 2$, be the change of variables from coordinates of the center manifold around L_i to the original ones of the QBCP.

The origin of the central coordinates is a fixed point of $H_{CM}^{(i)}$ that, by construction, corresponds to the small periodic orbit (5) (resp. (1)) around L_2 (resp. L_1). In the case of L_2, we have four additional fixed points in the plane $x_3 = 0$. Their coordinates and energy levels are shown in table VI. They have been labelled with the same label that their corresponding periodic orbits (6a)-(6d). From those periodic orbits of the QBCP, using the change of variables, we get points close to the fixed points of $H_{CM}^{(2)}$.

We want to comment that the fixed points (6a)-(6d) have the same stability character that their corresponding orbits. The points (6a) and (6c) are center×center. The other ones, (6b) and (6d), are saddle×center. All this, of course, inside the center manifold.

Besides the fixed points on the plane $x_3 = 0$, there are another four fixed points outside of the plane. They should correspond to the resonant Halo orbits of the QBCP, labelled as (7a) and (7c) (and the symmetric ones) in section 4. But, the location of these fixed points changes a lot when considering the Hamiltonian $H_{CM}^{(2)}$ up to order 12, 14 and 16. This suggests that those Halo orbits are too big and there the Hamiltonian $H_{CM}^{(2)}$ does not give a good approximation of the center manifold. The table VII shows the coordinates of one of the fixed points at different orders.

Table VI. Fixed points of $H_{CM}^{(2)}$ on the plane $x_3 = 0$. The fourth column shows the energy level $h = H_{CM}^{(2)}(x_1, y_1, 0, 0)$.

Label	x_1	y_1	h
6a	5.7778288e−02	5.7778292e−02	2.30211298e−05
6b	−6.6225712e−02	−4.5813575e−02	2.21256116e−05
6c	−5.6944434e−02	−5.6943907e−02	2.21256717e−05
6d	−4.5813275e−02	−6.6225920e−02	2.21256116e−05

Table VII. A fixed point outside the plane $x_3 = 0$ when $H_{CM}^{(2)}$ is taken up to orders 12, 14 and 16.

Order	$x_1 \simeq y_1$	$x_3 \simeq y_3$
12	9.4359e−02	2.9656e−02
14	9.1658e−02	2.5544e−02
16	8.9707e−02	2.2546e−02

In the xy plane around L_2, the change of variables ψ_2, as a function of time, is close to a rotation with frequency $2\omega_s$. For this reason, the periodic orbit with this frequency are seen as fixed points in the coordinates of the center manifold.

In the L_1 case, the change ψ_1 has as main frequency $3\omega_s$ in the xy plane and $2\omega_s$ in the z direction. The orbits (2a)-(2d) have frequency $5\omega_s/2$. Through the change ψ_1^{-1}, they map into a periodic orbit with frequency $3\omega_s - 5\omega_s/2 = \omega_s/2$. We note that cancelling the dependence on time we have lost some information. The orbits (2a)-(2d) and the stable and unstable invariant manifolds (inside de center manifold) of (2a) and (2c) correspond to a periodic orbit of H_{CM}. In some sense, H_{CM} shows an averaged dynamics and it has lost the tiniest details.

6. Checking the center manifold

In order to check all the computations done for the reduction to the central manifold, several tests have been implemented for different parts of the process. Here, we are going to talk about two checks involving the final Hamiltonian, H_{CM}, and the initial one, H_{QBCP}.

For the first check, we take an initial point in the central manifold, say $x_{cm}^{(0)}$. The Hamiltonian equations of H_{CM} are integrated with that

initial condition, for a time interval of 1, for instance. Let $x_{cm}^{(1)}$ be the point obtained. The point $x_{cm}^{(0)}$ can be transformed by the change of variables ψ_i obtaining $x_{qbcp}^{(0)}$ in the coordinates of the QBCP. Integrating the Hamiltonian equations of H_{QBCP} for a time span of 1 with initial condition $x_{qbcp}^{(0)}$, we get $x_{qbcp}^{(1)}$. This point can be transformed by ψ_i^{-1} obtaning $\tilde{x}_{cm}^{(1)}$. This point is expected to be close to $x_{cm}^{(1)}$. Let d be the distance between both points, which can be considered as a function of $x_{cm}^{(0)}$.

We remind that the orbits around L_1 and L_2 in the QBCP are highly unstable. If the initial conditions have some error, after the integration for a time interval of 1, that error is amplified by a factor about 10.

The distance d has been computed for several points in the central manifold along a straight line inside a level of energy. Figures 4a-f show the results for energy levels $h = 5\cdot 10^{-4}$, 0, $-5\cdot 10^{-4}$, along $x_1 = -y_1$, $x_3 = 0$, in the L_1 case and for energy levels $h = 10^{-5}$, 0, -10^{-5}, along $x_1 = y_1$, in the L_2 case. Similar plots can be done for other levels of energy or using another straight lines. The tests have been done using the Hamiltonian reduced to the central manifold up to several orders. We notice that, for large orbits, the results do not improve when increasing the order. That is related to the fact that the expansions are not convergent in any open set. However, the reduction to the central manifold up to order 12 for L_1 case and 16 for L_2 gives a good approximation of the dynamics in a neighbourhood of the libration points.

The second check of the center manifold consists in compare periodic orbits around L_i of the QBCP with the corresponding ones of the center manifold. For this check, we have used planar and vertical Lyapunov periodic orbits. In the L_1 case, we have computed orbits in resonaces $k : 709$, $k = 282, \ldots, 297$ for the planar family and $k : 515$, $k = 212, \ldots, 219$ for the vertical one. In the L_2 case, we have computed orbits in resonaces $k : 911$, $k = 454, \ldots, 467$ for the planar family and $k : 991$, $k = 514, \ldots, 522$ for the vertical one. It is necessary to use high order resonant orbits because the period of the orbits varies very slowly when increasing the size of the orbits. All these orbits have been computed from orbits of the RTBP, using parallel shooting method with several steps of a continuation method. Then, to check the accuracy of the reduction to the center manifold, we have computed periodic orbits of the $H_{CM}^{(i)}$ corresponding to the ones of the QBCP. The orbits of the $H_{CM}^{(i)}$ are transformed to the coordenates of the QBCP through the change of variables ψ_i. Say D_p the maximum difference of the components of the position and D_v of the velocity, for points of

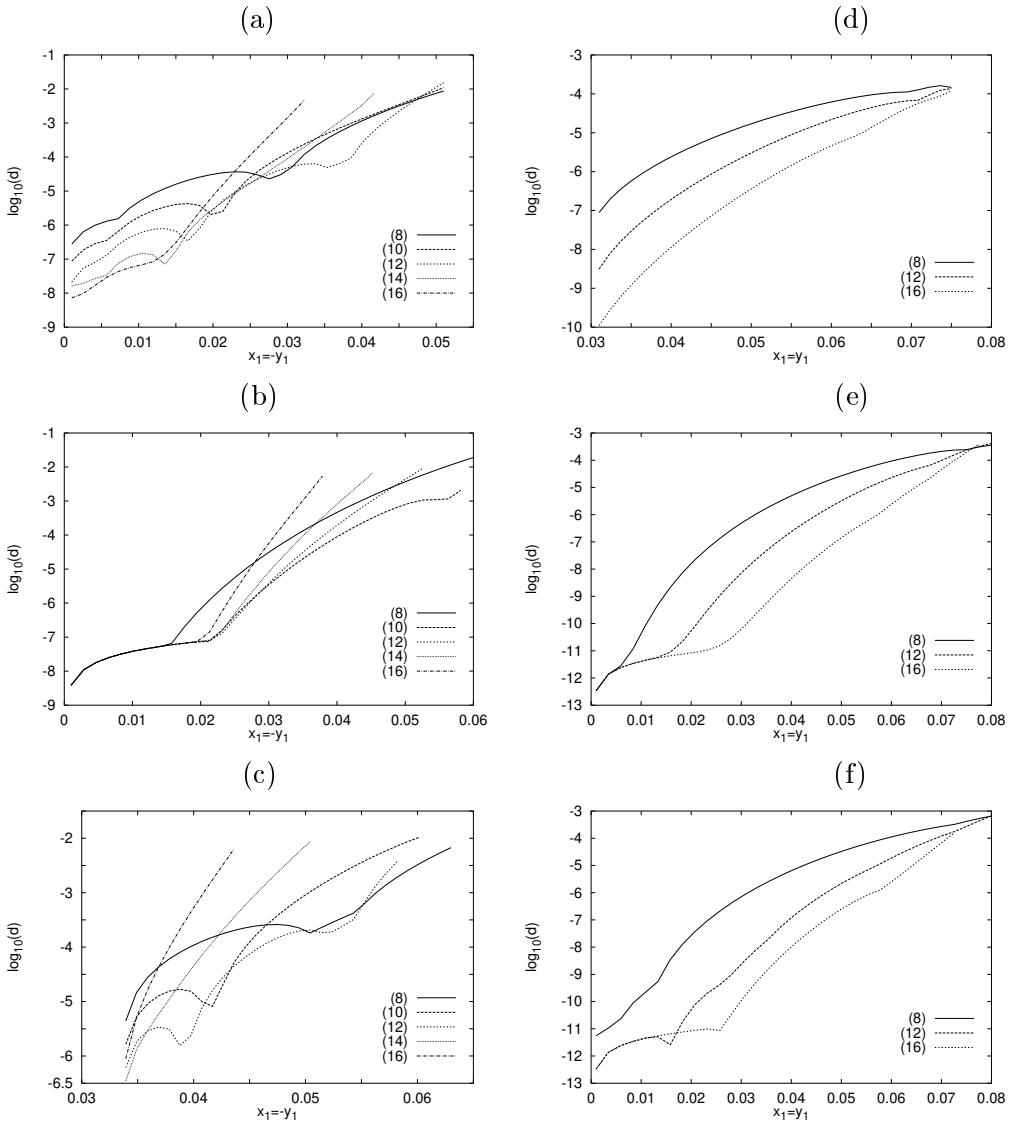

Figure 4. Results of the first test of accuracy. Around L_1 along $x_1 = -y_1$, (a) $h = 5 \cdot 10^{-4}$, (b) $h = 0$, (c) $h = -5 \cdot 10^{-4}$. Around L_2 along $x_1 = y_1$, (d) $h = 10^{-5}$, (e) $h = 0$, (f) $h = -10^{-5}$.

corresponding orbits at $t = 0$. Similar values can be obtained for other time values. Tables VIII and IX and figures 5 and 6 show the most representative results. For this test we have used $H_{CM}^{(1)}$ up to order 12 and $H_{CM}^{(2)}$ up to order 16. Figures 5 and 6 show zones with several levels of accuracy in the reduction to the center manifold.

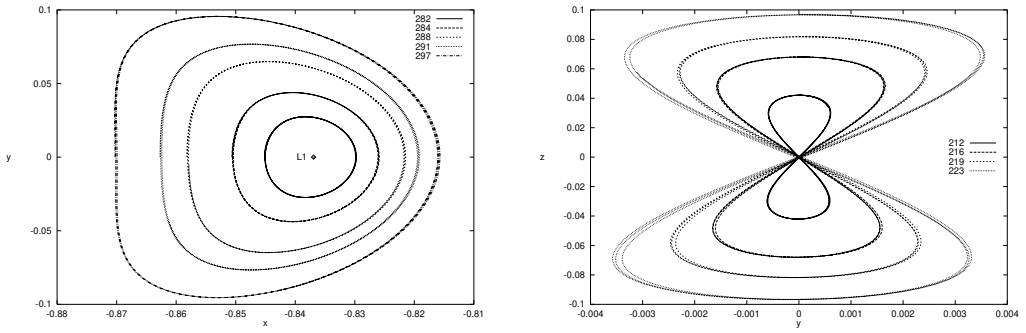

Figure 5. Planar and vertical periodic orbits around L_1 (see table VIII).

Table VIII. Test of periodic orbits for $H^{(1)}_{CM}$. The differences D_p and D_v are shown for some k : 709 resonant planar orbits and k : 515 for the vertical ones.

Planar Lyapunov			Vertical Lyapunov		
k	D_p	D_v	k	D_p	D_v
282	1.34e−07	1.01e−06	212	1.12e−07	4.41e−08
284	1.46e−06	1.02e−05	216	1.81e−06	1.74e−07
288	2.86e−05	1.86e−04	219	1.59e−05	3.48e−06
292	2.38e−04	1.51e−03	223	1.04e−04	3.09e−05
297	1.44e−03	8.86e−03			

7. Conclusions and outlook

The QBCP is a simple model for the motion on a spacecraft in the Earth-Moon-Sun system which is useful to understand the dynamics around de collinear libration points of the real Earth-Moon system.

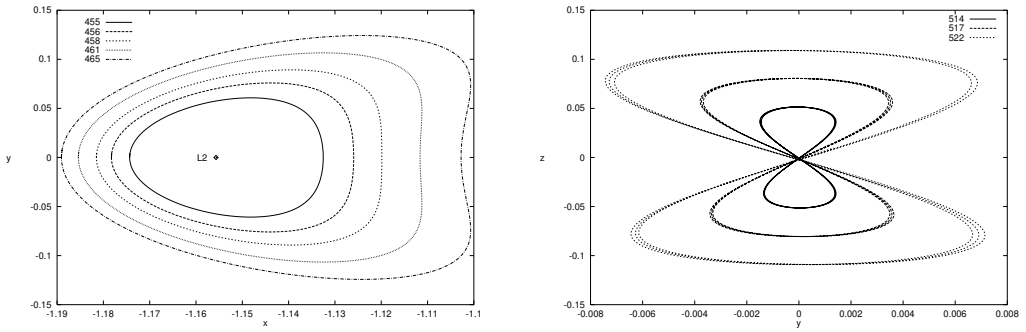

Figure 6. Planar and vertical periodic orbits around L_2 (see table IX).

Table IX. Test of periodic orbits for $H_{CM}^{(2)}$. The differences D_p and D_v are shown for some k : 911 resonant planar orbits and k : 991 for the vertical ones.

Planar Lyapunov			Vertical Lyapunov		
k	D_p	D_v	k	D_p	D_v
455	2.04e−10	6.27e−09	514	3.74e−05	2.07e−04
456	4.14e−07	2.99e−06	517	9.32e−05	5.24e−04
458	2.32e−06	1.78e−05	522	2.07e−04	1.01e−03
461	2.20e−05	1.80e−04			
465	1.69e−04	1.49e−03			

Presently, we are working in a full description of a neighborhood of L_1 and L_2 of the QBCP by means of the reduction of the Hamiltonian to the center manifold. Some results around L_2 were given in (Andreu, 1999). On the other hand, the families of Halo quasi-periodic orbits of the QBCP are being studied using a numerical method for the computation of invariant tori. Preliminary results of this work were shown in (Andreu et al., 1999b).

Acknowledgements

M.A. Andreu wishes to acknowledge the hospitality of the dept. of Matemàtica Aplicada I, Universitat Politèctina de Catalunya (Barcelona, Spain). C. Simó wants to thank the support of the spanish grant DGICYT PB94-215 and the catalan grant CIRIT 1998SGR-42.

References

Andreu, M.A.: 1998, *The Quasi-bicircular Problem*, Thesis, Dept. Matemàtica Aplicada i Anàlisi, Universitat de Barcelona.

Andreu ,M.A. and Simó, C.: 1999a, 'Translunar Halo orbits in the Quasi-bicircular Problem', B.A. Steves and A.E. Roy editors, *The Dynamics of Small Bodies in the Solar System*, NATO ASI (1997, Maratea, Italy), pp. 309-314.

Andreu, M.A. and Simó, C.: 1999b, *Estudio de la estabilidad de una familia de toros 2D del problema Cuasibicircular*, XVI CEDYA/VI CMA, (1999, Las Palmas de Gran Canaria, Spain), Vol. I, pp. 131-138.

Farquhar, R.W.: 1970, *The Control and Use of Libration-Point Satellites*, NASA TR R346.

Gómez G., Llibre J., Martínez R. and Simó C.: 1987, *Study on orbits near the triangular libration points in the perturbed restricted three body problem*, ESOC contract 6139/84/D/JS(SC), Final Report.

Jorba À.: 1999, *On practical stability regions for the motion of a small particle close to the equilateral points of the real Earth-Moon system*, (preprint).

Jorba À., Llave R.: *Regularity properties of center manifolds and applications* (in preparation).

Kolenkiewicz, R. and Carpenter, L.: 1968, 'Stable periodic orbits about the Sun perturbed Earth-Moon triangular points', AIAA 6, 1301-1304.

Marchal, C.: 1990, *The Three-Body Problem*, Elsevier.

Mohn, L. and Kevorkian, J.: 1967, 'Some limiting case of the restricted four body problem', *Astron. Jour.* **72**, 959-963.

Scheeres, D.J. and Vinh, N.X.: 1992, 'The Restricted Hill Four-Body Problem', 43rd *Congress of the International Astronautical Federation*, Washington.

Siegel, C. and Moser, J.K.: 1971, *Lectures notes in Celestial Mechanics*, Springer-Verlag, New York.

Simó, C.: 1990, 'Analytical and numerical computation of invariant manifolds'. In D. Benest et C. Froeschlé, editors, *Modern methods in celestial mechanics*, pag. 285-330, Editions Frontières.

Stoer, J. and Bulirsch, R.: 1980, *Introduction to numerical analysis*, Springer-Verlag.

Wiesel, W.: 1984, *The restricted Earth-Sun-Moon problem I: Dynamics and libration point orbits*, Dept. Aeron. and Astron., Air Force Institute of Technology Wright-Patterson AFB, Ohio.